Near-Field Scanning Optical Microscopy of Single Fluorescent Dendritic Molecules

Joost A. Veerman,[†] Stefano A. Levi,[‡] Frank C. J. M. van Veggel,[‡] David N. Reinhoudt,*[,‡] and Niek F. van Hulst*[,†]

Applied Optics Group, and Laboratory of Supramolecular Chemistry and Technology, MESA+ Research Institute, University of Twente, P.O. Box 217, 7500 AE Enschede, The Netherlands

Received: July 28, 1999; In Final Form: September 29, 1999

Individual dendritic molecules adsorbed on glass containing a single fluorescent rhodamine B core have been observed with near-field scanning optical microscopy (NSOM); height and fluorescence images were obtained simultaneously. The dendritic assemblies can be discriminated from free fluorescent cores on the basis of accurate simultaneous localization of both the fluorescent core and the surrounding dendritic shell. There are no significant differences between the photophysical properties of the free and dendritic fluorophores. The full three-dimensional orientation of each individual fluorescent core can be resolved and millisecond time resolution accuracy has been achieved. Most dendritic structures exhibited rotational motion of the fluorescent core on a millisecond−second time scale, revealing intramolecular conformational dynamics.

Introduction

Nanochemistry is a rapidly expanding field that requires synthesis, characterization, and manipulation of nanosize structures.[1] In contrast to conventional physical "top-down" approaches, e.g., electron-beam lithography, chemistry follows a "bottom-up" approach through which molecular building blocks are connected to complex structures of nanometer dimensions.[2]

In this paper, we report the synthesis of dendritic molecules containing a single fluorescent rhodamine B (RhB) core and their observation at the single-molecule level with near-field scanning optical microscopy (NSOM). Dendritic molecules are regular hyperbranched polymers that originate from a core by means of repetitive reactions. With dimensions from few to hundreds of nanometers, they are ideal "molecular platforms" to attach functional groups in well-defined three-dimensional architectures.

Detection of individual molecules reveals the full distribution of molecular parameters, whereas detection of an ensemble of molecules only yields average values. Moreover, at the single-molecule level, phenomena such as rare transitions to metastable states and rotational and spectral jumps otherwise hidden in the ensemble can be observed.[3] In comparison to far-field optical microscopy, NSOM offers the unique advantage of superior optical subwavelength resolution and simultaneous height information. Previously, we[4,5] and others[6,7] have shown that the nanometer scale colocalization capability of NSOM is excellently suited to study individual molecules. Recently, detection of single dendrimers with a fluorescent core embedded in a thin polystyrene film was accomplished by Hofkens et al. using confocal microscopy.[8]

In this paper, we report the first simultaneous measurement of topography and fluorescence of single dendritic molecules adsorbed on a glass surface.

Experimental Section

All chemicals were purchased from Aldrich and Molecular Probes and were used without further purification. Syntheses were carried out under an argon atmosphere. ^{1}H and ^{13}C spectra were recorded in $CDCl_3$ on a Varian Inova NMR spectrometer, operating at 300 and 75.5 MHz for ^{1}H and ^{13}C, respectively. Residual solvent protons were used as the internal standard, and chemical shifts are given in ppm relative to tetramethylsilane (TMS). Absorption and emission fluorescence spectra of the dendritic molecules dissolved in nitromethane were obtained on a SPF-500 spectrofluorometer. IR spectra were recorded in CH_3NO_2 solution on a BIORAD IR spectrophotometer. Atomic force microscopy (AFM) images in tapping mode were obtained on both a home-built system optimized for high scan speed and low height noise[9] and a DI NanoScope IIIa. NSOM was performed on a home-built system with a polarization-sensitive detection scheme, as described elsewhere.[10] Height tracking of the sample was accomplished with a 0.2 nm residual noise feedback scheme based on a tuning fork for shear-force detection. Homemade high-definition focused ion beam (FIB) modified probes were used, combining high throughput and excellent imaging of polarization characteristics.[11] The RhB core molecules were excited at 514 nm with typically 1 kW/cm^2 excitation intensity. Fluorescence was collected with a 1.3 NA objective, filtered with a long-pass filter at 550 nm, separated by a broadband polarizing beam splitter in two orthogonal polarization channels and detected with two photon-counting avalanche photodiodes. A fluorescence signal of typically 50 kcounts/s was detected from an individual RhB core molecule. Three images of the sample were obtained simultaneously: one height image and two optical fluorescence images. Optical images were false-colored with a red scale for the *x*-polarization detection channel and a green scale for the *y*-polarization detection channel.

Results and Discussion

First, we will introduce the synthesis route we used. Thereafter, we present NSOM topographic and optical images, which illustrate colocalization and orientation determination of single dendritic molecules. In the last part of the paper, we discuss reorientation dynamics of fluorescent cores.

Synthesis. We have previously shown that it is possible to build large organopalladium spheres using coordination chem-

* Corresponding authors. E-mail: first, n.f.vanhulst@tn.utwente.nl, and second, d.n.reinhoudt@ct.utwente.nl.
[†] Applied Optics Group.
[‡] Laboratory of Supramolecular Chemistry and Technology.

10.1021/jp992635u CCC: $18.00
Published on Web 12/03/1999

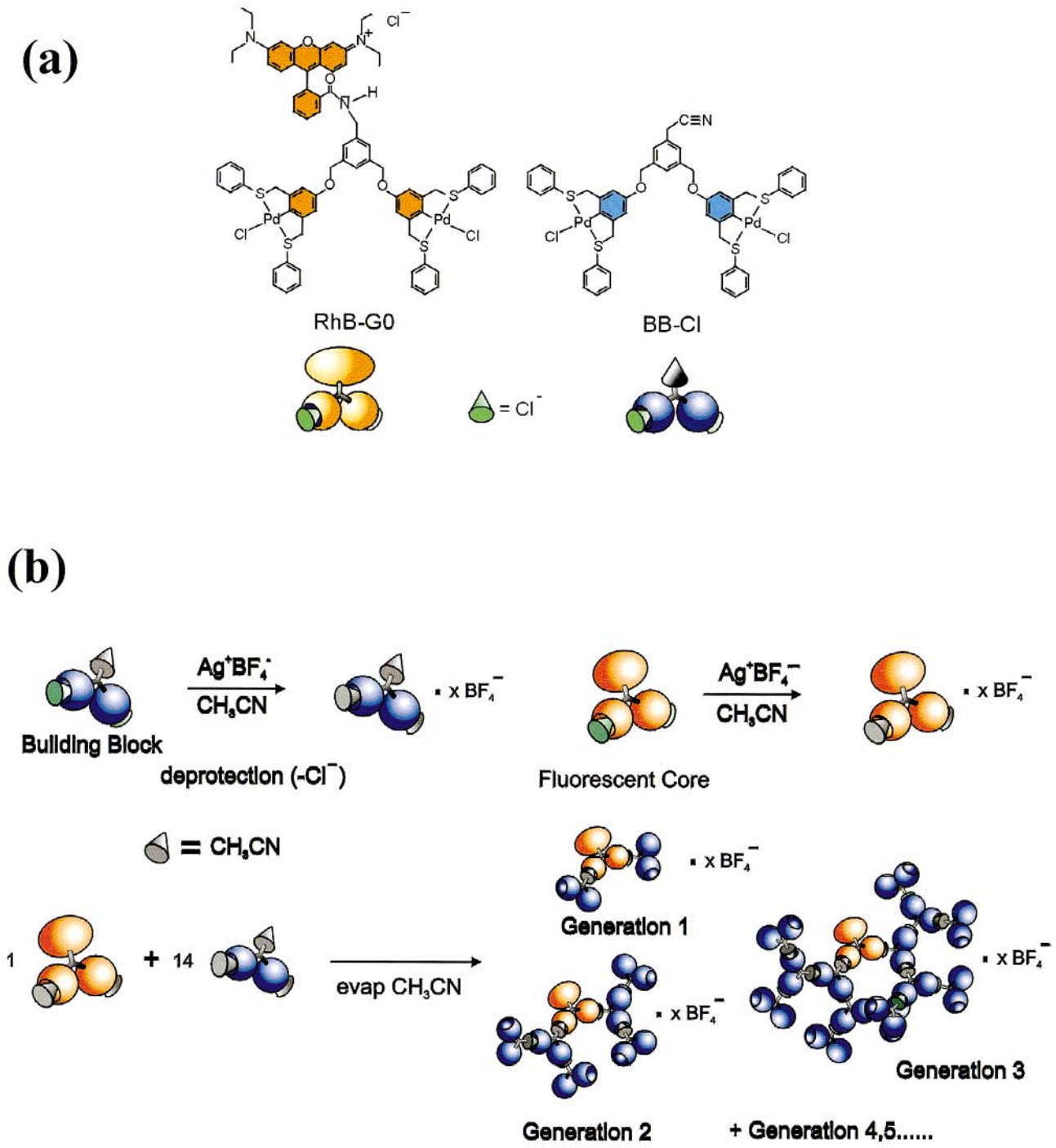

Figure 1. (a) Fluorescent core unit (RhB-G0) and building blocks (BB−Cl) and (b) assembly of the dendritic molecules.

istry.[12] Compound BB−Cl (Figure 1a) can be used as building block for the genuine assembly of dendritic structures. After removal of the chloride, coordinated to the 4th coordination position of the palladium, upon addition of a stoichiometric amount of $AgBF_4$, each building block coordinates two molecules of acetonitrile. Evaporation of the solvent yields dendritic spheres with varying size depending on the size of the counterion used (100−150 nm in the case of BF_4^-).[13,14]

In this work, we use a similar procedure, but it is based on the assembly of two components (Figure 1a). Compound RhB-G0 acts only as core containing the fluorescent function, and BB−Cl, the chloride-protected building block, is used to grow different dendritic molecule generations around the core. Full details about the synthesis and properties of the fluorescent core will be published elsewhere. The absorption and emission maxima peak at 555 and 580 nm, respectively.

The two deprotected components were dissolved in acetonitrile in a ratio of 1:14 (core: BB−Cl) (Figure 1b). By use of this ratio, a random size distribution of dendritic molecules is expected with a molecular distribution that has a maximum at generation three. Upon evaporation of acetonitrile, it was possible to obtain organopalladium spheres containing only one fluorescent core per molecule.

The polydispersed dendritic molecules were characterized by IR spectra: ν 2292 cm^{-1} corresponds to stretching of Pd-coordinated nitrile groups. There is no absorption at 2259 cm^{-1} corresponding to free nitrile groups, which indicates complete coordination of the building blocks. ^1H NMR in CD_3NO_2

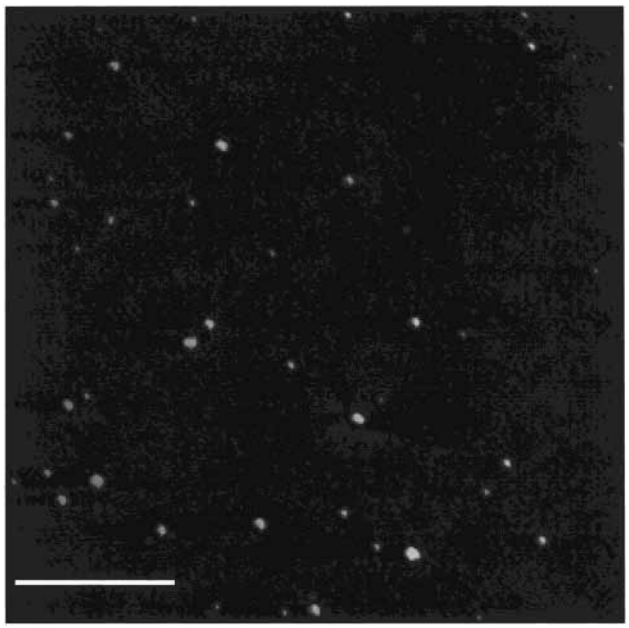

Figure 2. Dynamic mode AFM image ($2 \times 2\ \mu m^2$) showing dispersed spheres corresponding to individual dendritic molecules adsorbed on a glass surface, with a mean height of 7.5 ± 0.5 nm and a mean width of 21 ± 1 nm. Scalebar: 500 nm.

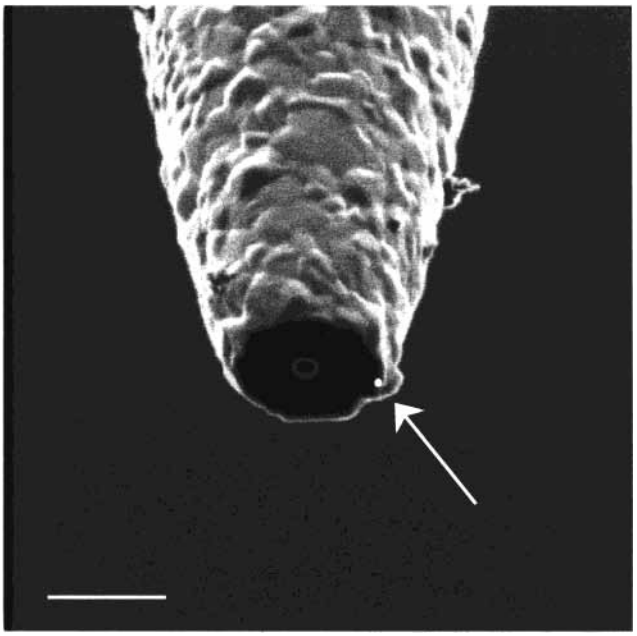

Figure 3. Focused ion beam (FIB) image recorded after side-on milling of the 70 nm aperture NSOM probe that was used for the measurements. The white dot indicates the position of the shear-force sensing local protrusion at the edge of the end-face. Scalebar: 500 nm.

showed broad spectra, indicating the presence of large assemblies, and addition of small amounts of CH_3CN gave spectra with the sharp peaks of the individual components.[14]

Characterization with AFM. The size and polydispersity of the spheres were obtained using AFM. A solution of dendritic molecules in nitromethane (10^{-8} M) was spin-coated on glass, to yield a sample with several tens of molecules per μm^2. Figure 2 shows the AFM dynamic mode height image of such a sample of $2 \times 2\ \mu m^2$. The isolated spheres in the image may correspond to individual dendritic molecules or small clusters.

The height distribution of the dendritic molecule spheres exhibits a Poissonian shape with a height value of 7.5 ± 0.5 nm and a fwhm of 5.0 ± 0.5 nm. The lateral diameter of the spheres varies between a lowest value of 13 nm (limited by the AFM tip convolution) up to 40 nm with a peak size of 21 ± 1 nm. The Poissonian peak height distribution shows dendritic structures of different sizes. The peak height of 7.5 nm matches a generation 3 assembly, as expected from the ratio of 1:14 between core and building block used in the synthesis.

Co-localization with NSOM. In comparison with AFM, NSOM provides the benefit of additional optical information. We have already shown that with NSOM individual fluorescent molecules can be localized with an accuracy of $\sim$1 nm.[10] As the dendritic molecules have been labeled with one single fluorescent core, optical detection with NSOM yields a unique opportunity to correlate single-molecule fluorescence on the surface with an individual dendritic molecule. Moreover, polarization sensitive detection can be used to distinguish a single molecule from a cluster. The orientation of the dipole moments of the fluorescent cores in a cluster will be randomly distributed, giving rise to unpolarized fluorescence emission. On the other hand, single-molecule fluorescence will be polarized in the direction of the emission dipole.

Figure 3 shows a FIB image of the aluminum coated probe with a 70 nm aperture diameter that was used for all NSOM measurements described in this paper. Figure 4a displays an NSOM shear-force height measurement of a $1.65 \times 1.65\ \mu m^2$ area of the same sample of the AFM image in Figure 2, using the probe depicted in Figure 3. The probe was scanned line-by-line in the horizontal image direction, starting at the top left corner. Both isolated and agglomerated spheres are visible in the image. The isolated spheres have a minimum fwhm of 20 nm, whereas the lateral cluster size ranges up to several hundreds of nm. Within the clusters, individual spheres can be resolved with the same typical size as the isolated spheres. The height of the spheres is between 5 and 7 nm, which closely matches the distribution found by AFM height measurements. The typical lateral diameter of the spheres in this shear-force image is of the same order as found with AFM. The correspondence of the height distributions obtained with dynamic mode AFM and shear-force mode NSOM is of crucial importance, as the tip−sample interaction and hence the contrast mechanism are different in both methods. Therefore, despite the difference in geometrical shape, size and material between an AFM and an NSOM tip, both methods effectively probe a reliable height distribution of the sample.

Simultaneously with the shear-force image, an NSOM fluorescence image was obtained (Figure 4b). The excitation at 514.5 nm was circularly polarized (as measured in the far-field). The colors in the image correspond to the polarization direction of the detected fluorescence, ranging from green (polarization in the vertical image direction) through yellow (unpolarized light or polarization at $\pm 45°$) to red (horizontal polarization). Besides isolated spots, representing individual emitters, larger agglomerates with an overall yellow color can be distinguished. Comparison with the shear-force image in Figure 4a directly shows that the agglomerates correspond to the dendritic molecule clusters. To facilitate a better analysis, both images are plotted on top of each other in Figure 4c. Indeed, a strong correlation is present between spheres, clusters of spheres, and the presence of fluorescence.

Figure 5 illustrates the resolution difference between the height and optical images of the dendritic molecules. Because the end-face of the NSOM probe is flat over a few hundred nanometers, a much smaller protrusion forming a "supertip" acts as the actual shear-force sensing element (see Figure 5a).

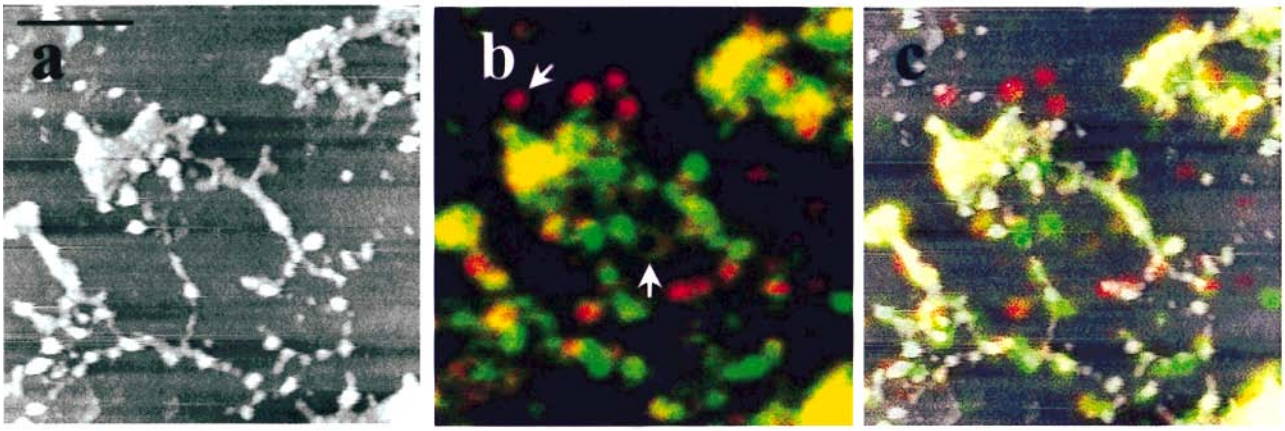

Figure 4. (a) NSOM shear-force image ($1.65 \times 1.65\ \mu m^2$) showing both isolated and clustered dendritic molecules on a glass surface. Scalebar: 450 nm. (b) Simultaneously obtained fluorescence image, with ~70 nm optical resolution. Circularly polarized excitation light at 514.5 nm was used. A false-color scale indicates the polarization of the fluorescence (red, horizontal image direction; green, vertical image direction) and thus the in-plane orientation of the molecular emission dipole. (c) Combined shear-force (gray scale) and fluorescence (red−green color scale) image (*a* + *b*) illustrating the correlation between height and optical signals.

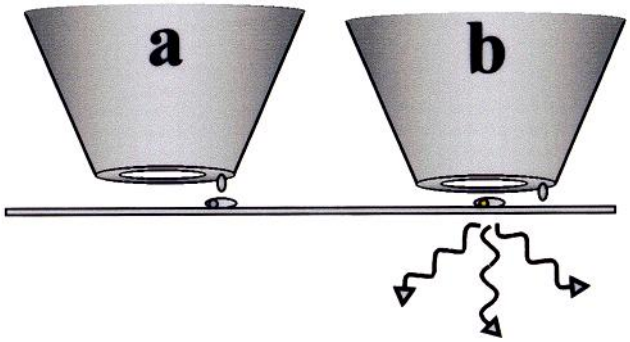

Figure 5. (a) Schematic view of the height tracking of an adsorbed dendritic molecule by a local protrusion on the NSOM probe and (b) the optical imaging of the fluorescent core-unit by the aperture.

The absolute position and size of the supertip is indicated in Figure 3 by the white dot at the right side of the end-face (arrow). The resulting convolution of this supertip with the adsorbed dendritic molecules is about twice the size of the AFM-tip convolution with the molecules. On the other hand, the optical resolution is solely determined by the aperture size (see Figure 5b). All NSOM images in this paper were corrected for the displacement caused by the distance between supertip and aperture. As a consequence, knowledge of this systematic shift in combination with the optical localization accuracy of ~1 nm facilitates a determination of the fluorescent core position within the adsorbed molecule.

Several observations support the identification of the isolated fluorescence spots as single dendritic molecules: (i) the spots typically display well-defined polarized emission, which implies one fixed dipolar emission moment; (ii) they exhibit an abrupt termination of the emission (probably due to photodissociation) after repeated scans; (iii) they show discrete on−off blinking of the fluorescence on a millisecond−second time scale, probably due to temporal excursions to a metastable state; and (iv) the emission signal is on the same order of magnitude as the signal that was obtained with the same NSOM probe from a reference sample of single $DiIC_{18}$ molecules in a PMMA thin film. In the dendritic molecule clusters, several molecules are illuminated simultaneously by the NSOM probe, resulting in a higher signal level than the isolated spots and randomized polarization, as confirmed by using different excitation polarization conditions. Because of the small illumination volume of the NSOM probe, at some positions individual molecules can still be distinguished optically within the cluster areas.

Figure 4c clearly illustrates the close match between the shear-force height image and the optical image. However, a precise look reveals that some spherical particles in the shear-force image do not exhibit any fluorescence. We can exclude the possibility that these fluorophores are not excited, because the chosen excitation polarization, in combination with the high-definition FIB-modified NSOM probe, ensures the presence of an optical field polarization component in all spatial directions. Several explanations can be given for the absence of fluorescence for some dendritic molecules: (i) those particular molecules may not have a fluorescently labeled core; (ii) the fluorescent core could have been photobleached previously; and (iii) the fluorescent core could be in a nonfluorescent state.

Conversely, some fluorescent spots in the optical image (Figure 4b) do not correspond to any height features in the shear-force image (Figure 4a). We attribute these fluorescent sites to core molecules or lower generations that are too small to be detected by the NSOM shear-force mechanism. Whereas AFM cannot resolve these small chromophoric units in height either, NSOM allows identification of such molecules by the sensitive photon-counting fluorescence detection.

The presence of both fully assembled dendritic molecules containing a fluorescent core and unreacted fluorescent core molecules allows a comparison of their rotational activity and photophysical behavior. For these particular dendritic structures, we find no significant differences in intensity, dissociation behavior, and temporal intensity jumps (blinking) in comparison with free cores. Consequently, the photophysics of the fluorescent core unit is not substantially altered upon assembly in the dendritic structure.

Intramolecular Rotational Movements. Rotational movements of single molecules can be monitored with NSOM in two different ways. One method is to determine the orientation of the emission dipole by measuring the polarization of the fluorescence. The second way is to find the absorption dipole moment orientation using the electric near-field distribution of an NSOM probe. The first method is only sensitive for the in-plane component of the emission dipole, whereas the latter also probes perpendicularly oriented absorption dipoles. In our measurements, we combined both methods to monitor both the absorption and emission dipole orientation as a function of time.

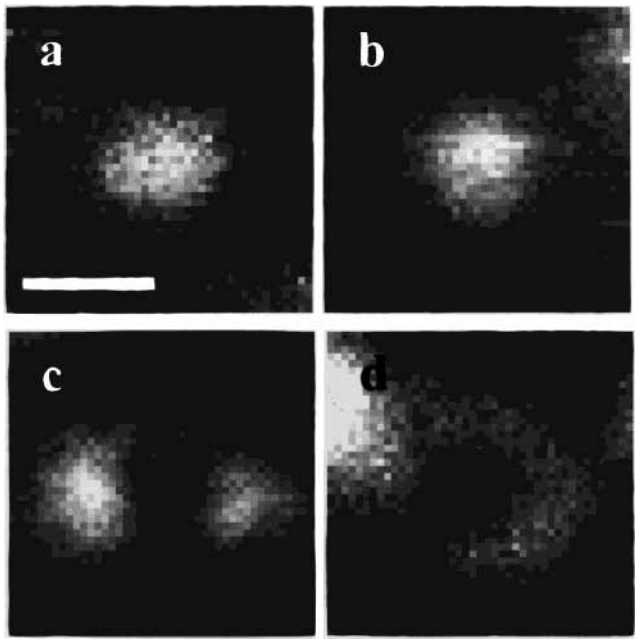

Figure 6. Characteristic NSOM single-molecule emission patterns (obtained with the 70 nm aperture probe of Figure 3) for in-plane absorption dipole orientations in the (a) horizontal and (b) vertical image direction and out-of-plane tilted absorption dipole orientations excited with (c) linear and (d) circular polarized light. The resolution varies from 65 to 90 nm fwhm for the elliptical in-plane molecule patterns to 45 nm fwhm for the double-lobed and ringlike patterns. Scalebar: 120 nm.

The sensitivity of NSOM for the absorption dipole orientation is illustrated in Figure 4b, which shows differences in shape among various isolated fluorescent spots. It is well-known that the near-field distribution of an NSOM aperture has electric field components in all directions.[15−17] Thus, a full three-dimensional orientation determination of the absorption dipole becomes feasible.[18,19] In-plane polarization components are mainly present in the center of the aperture, whereas polarization components perpendicular to the aperture plane are present at the rims. Consequently, whereas the color in Figure 4b is an indication for the in-plane emission dipole orientation of the fluorescent core within the dendritic molecule, the shape of the molecular image is connected to its absorption dipole orientation. For example, an elliptical shape like the red molecule in the left upper corner of Figure 4b indicates a planar orientation of the absorption dipole, whereas a ringlike shape such as the marked molecule in the center of the image indicates a perpendicularly oriented absorption dipole. The fwhm of the elliptical spots is between 65 and 90 nm (short and long axis, respectively), and the inner core diameter of the ringlike spot is 70 nm, which closely matches the expected resolution for a 70 nm aperture at a distance of ∼25 nm.[15,16,19] Different optical molecular imaging patterns that were found on the fluorescent dendritic molecule sample are shown in Figure 6a−d. Depending on the absorption dipole orientation, the shape changes from elliptical for planar oriented dipoles (Figure 6a, *x*-direction; Figure 6b, *y*-direction) to double-lobed (Figure 6c) or ringlike (Figure 6d) for a perpendicular orientation (excited with linear and circular polarization, respectively).[18,19]

We did not observe a preferential direction of the emission dipole of the fluorescent dendritic molecules. Therefore, probably no specific adsorption sites are present within the dendritic shell. Surprisingly, we observe rotational activity of both free and assembled fluorescent cores on a millisecond−second time scale. To our knowledge, it is the first direct observation of guest mobility within a surrounding host for a single molecule.

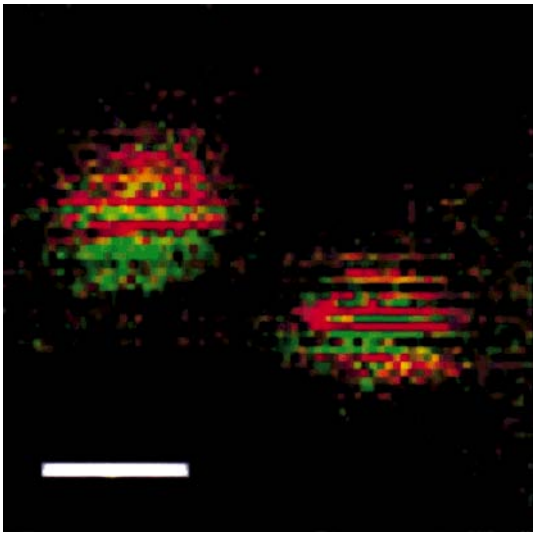

Figure 7. Emission dipole rotational movements (visualized by the red−green transitions) of a fluorescent dendritic molecule (left pattern) and a free fluorescent core unit (right pattern). Rotations occur on a millisecond−second time scale (pixel dwell time, 5 ms; time between successive lines, 4 s). Scalebar: 110 nm.

Figure 7 shows an optical image obtained with circularly polarized excitation of a 400 × 400 nm^2 area with two fluorescent molecules lying ∼200 nm apart. A comparison with the corresponding shear-force image revealed that the left molecule corresponds to a dendritic molecule and the right one to a smaller fluorescent assembly. Both molecules exhibit temporal changes in their in-plane emission dipole orientation, as visualized by the color changes from red to green. Between orientational jumps, the dipole position remains constant for periods ranging from the order of milliseconds (typical pixel time resolution) to seconds (time between successive lines).

Figure 8a−d shows more complex dynamical behavior in a series of four successive combined shear-force and optical images of the same 750 × 750 nm^2 area. As in Figure 4c, the shear-force image is plotted in gray scale on top of the false-color-coded optical image. The time between two images is approximately 30 min. The excitation polarization (as measured in the far-field) was linear along the horizontal image direction (*x*-direction, red detection channel) in Figure 8a, linear along the *y*-direction in Figure 8b-c, and circular in Figure 8d. Several dendritic molecules and clusters of molecules can be recognized in gray scale, a part of them are correlated with fluorescence signal. Again, as in Figure 4, some dendritic molecules are not fluorescent, and some fluorescent spots do not correlate with a dendritic molecule.

We now want to focus on the molecular reorientations that are visible in and between these images. We will concentrate on two characteristic regions within the images, which have been marked in Figure 8a. The fluorescence of the molecule in region 1 exhibits a strong on−off behavior (Figure 8a−c). Such on−off switching is well-known for many single quantum emitters, such as organic dyes and semiconductor nanocrystals.[3] Discrete emission intensity jumps may be explained by a number of possible inter- and intramolecular photophysical mechanisms. For example, transitions to a long-lived metastable state or sudden jumps of the spectrum or quantum yield could occur. However, in Figure 8 the temporal interruption of fluorescence is primarily caused by molecular reorientations. Especially, the fact that the "color" of the fluorescence pattern (and thus the

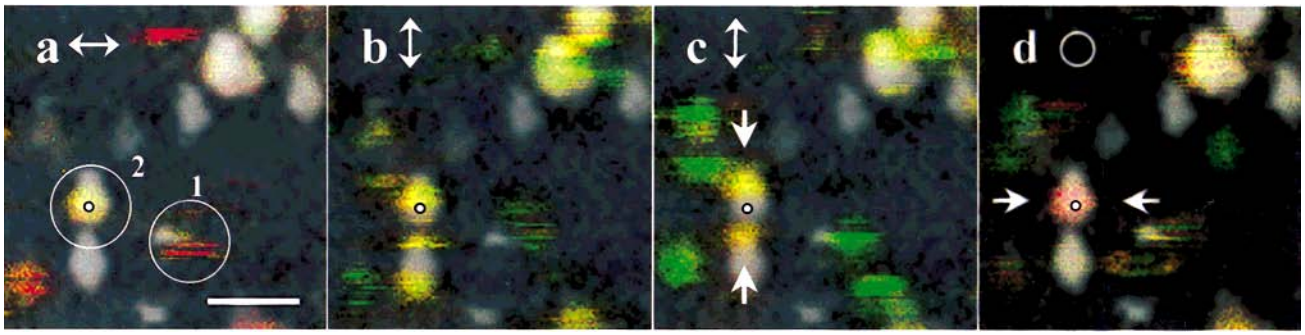

Figure 8. Series of four successive combined shear-force (gray scale) and fluorescence (red−green false-color scale) images of the same area (750 × 750 nm^2) obtained with different excitation polarization conditions ((a) linear along *x*, (b, c) linear along *y*, and (d) circular), showing in- and out-of-plane reorientations of single dendritic molecules. The white dots indicate the positions of some of the molecules that change appearance between images (see text for detailed discussion). Scalebar: 210 nm.

orientation of the molecule) changes from red in Figure 8a (with the excitation polarization along the "red" direction) to green in parts b and c of Figure 8 (with corresponding "green" excitation polarization) suggests that the core indeed rotates. The molecule will only be excited if the absorption dipole is collinear with the near-field excitation polarization direction. As the absorption and emission dipole moments are collinear as well, the emission will be preferentially polarized along the excitation polarization direction. In Figure 8a−c, any in-plane orientation of the molecular dipole away from the excitation polarization diminishes the fluorescence yield. However, if circularly polarized excitation light is used (as in Figure 7), in-plane rotations will not lead to modulation of the fluorescence intensity, but to anticorrelated behavior of the signals in both detection channels. Indeed, such red−green jumps can be recognized in Figure 8d where circularly polarized excitation light was used.

Out-of-plane reorientations are observed for the molecule in region 2. In Figure 8a, the molecular fluorescence pattern is circular and yellow-colored, which indicates a major in-plane orientation at about 45° to the detection channels. However, the pattern changes to a double-lobed configuration in Figure 8c, which is characteristic for a mainly perpendicularly oriented dipole. Figure 9a shows line traces of the fluorescence signal over this pattern along the direction indicated by the arrows in Figure 8c. Two adjacent lines are shown to illustrate the reproducibility of the pattern. The dark region in the middle is caused by the absence of perpendicularly oriented electric fields in the center region of the aperture of the NSOM probe. Only at the rims of the aperture are those fields present, leading to fluorescence peaks with a fwhm of 45 nm. Such an optical resolution very closely approaches the dendritic molecule dimensions in the topographical shear-force or AFM images, reflecting the physical size of the molecules. Note that a far-field imaging pattern of this molecule would have taken almost the entire 750 × 750 nm^2 area of the figure. The same molecule changes its appearance again in Figure 8d, where the horizontal elliptical pattern is an indication for an in-plane orientation along the *x*-direction. Figure 9b displays the fluorescence signal of the molecule along lines between the arrows in Figure 8d. The fwhm of 85 nm along the long axis of the elliptical patters (fwhm short axis, 65 nm) is determined by the 70 nm aperture size and the distance between aperture and molecule of ~25 nm. In contrast to the molecule in region 1, the molecule in region 2 is stable within each image (except for some rotations in Figure 8b). Accordingly, its orientational movements are restricted to a lower rate than those of the molecule in region 1.

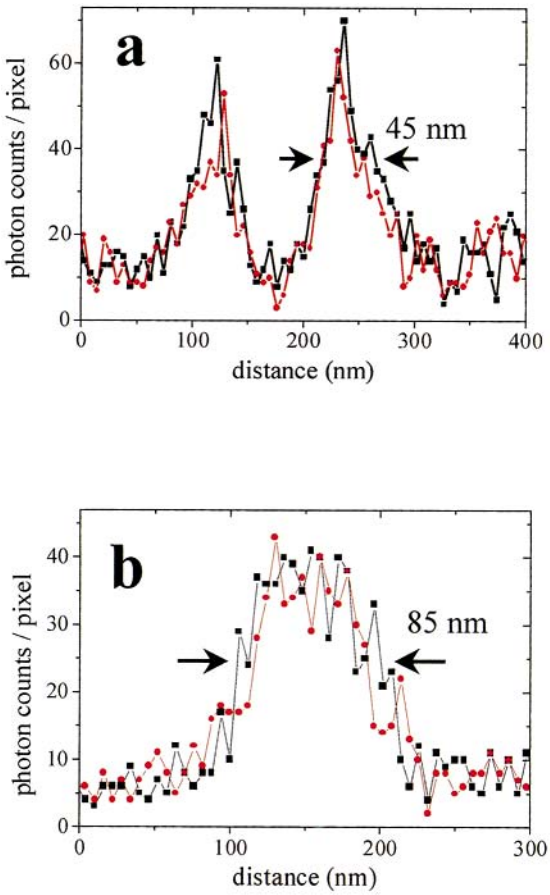

Figure 9. Fluorescence linetraces of the same molecule in two different orientations, taken from adjacent lines (colored red and black) in Figure 8c (a) and Figure 8d (b) (see arrows), showing (a) a double-lobed emission pattern with a fwhm of 45 nm and (b) an elliptical pattern with a fwhm of 85 nm, respectively. Thus, the absorption dipole is tilted out of plane in part a and has an overall in-plane orientation along *x* in part b.

Single-molecule rotational movements have been previously observed for, e.g., dye−DNA complexes linked to a silica substrate and within dye-doped polymer systems.[4,10,20] For the dye−DNA complexes, rotational movements were attributed to the flexible DNA-linking between dye and surface. Orientational jumps in polymer environments have been related to low-frequency polymer side-group motions. In the measurements presented here, orientational changes of the emission dipole occur much more frequently than those in the above-mentioned cases. Therefore, it is unlikely that the entire molecular assembly is involved in the observed motions. In neither the AFM nor

the NSOM shear-force height images could such events be detected. Continuous monitoring of the fluorescence with the probe stationary above a molecule revealed the same orientational movements, which excludes possible probe-induced effects.

Hence, we observe motional freedom of the fluorescent core unit within the assembly. The fluorescent core is attached to the dendritic shell via coordinated palladium bonds, which allow certain motional degrees of freedom. In contrast to our observations, recent measurements of single dendrimers embedded in a thin polystyrene film revealed only small rotational movements on a much longer time scale (tens of seconds), probably caused by thermally induced polymer movements.[8] Both the assembly (coordinative vs covalent bonds) and the environment (polymer vs glass-air interface) account for the different orientational dynamics in both measurements. The internal structure and the local environment of the polymer-embedded molecules provide a larger rigidity of the assembly, which probably induces smaller and slower reorientation dynamics compared to our system.

Conclusions

For the first time, NSOM measurements on single fluorescent dendritic molecules have been performed. Height and optical images of individual molecules were obtained simultaneously, which allowed colocalization of single-molecule fluorescence with dendritic molecules. In this way, nonfluorescent dendritic molecules and fluorescent assemblies with varying size could be discriminated. Such a differentiation is highly beneficial for any detailed investigation at the single-molecule level of dendritic photophysics. The accuracy for localizing the fluorescent core position is as good as 1 nm, which implies that even the core position relative to the immobilized dendritic assembly can be determined. No differences were found in the dendritic molecule height distribution obtained with dynamic mode AFM and shear-force NSOM, which emphasizes the nondestructiveness of both techniques. No significant differences were found between the photophysical behavior of the free and assembled fluorescent units. The three-dimensional orientation of the individual fluorescent cores within the dendritic host could be determined. For the first time, orientational mobility of guest units within a molecular host shell has been observed, which demonstrates the ability of single-molecule detection to reveal dynamical behavior in a complex environment at the nanometer scale.

Acknowledgment. We acknowledge the Dutch foundation for fundamental research on matter (FOM) and the Nanolink Program of the MESA$^+$ Research Institute for financial support of this work. We thank John van Noort for the AFM images.

References and Notes

(1) Ozin, G. A. *Adv. Mater.* **1992**, *4*, 612.
(2) Huck, W. T. S.; van Veggel, F. C. J. M.; Reinhoudt, D. N. *Angew. Chem., Int. Ed. Engl.* **1996**, *35*, 1213.
(3) Basché, T., Moerner, W. E., Orrit, M., Wild, U. P., Eds. *Single-Molecule Optical Detection, Imaging and Spectroscopy*; VCH: Weinheim, 1997.
(4) Garcia-Parajo, M. F.; Veerman, J. A.; van Noort, J.; de Grooth, B. G.; Greve, J.; van Hulst, N. F. *Bioimaging* **1998**, *6*, 43.
(5) Garcia-Parajo, M. F.; Veerman, J. A.; Segers-Nolten, G. M. J.; de Grooth, B. G.; Greve, J.; van Hulst, N. F. *Cytometry* **1999**, *6*, 239.
(6) Dunn, R. C.; Allen, E. V.; Joyce, S. A.; Anderson, G. A.; Xie, X. S. *Ultramicroscopy* **1995**, *57*, 113.
(7) Bopp, M. A.; Meixner, A. J.; Tarrach, G.; Zschokke-Granacher, I.; Novotny, L. *Chem. Phys. Lett.* **1996**, *263*, 721.
(8) Hofkens, J.; Verheijen, R.; Shukla, R.; Dehaen, W.; De Schryver, F. C. *Macromolecules* **1998**, *31*, 4493.
(9) Van der Werf, K. O.; Putman, C. A.; de Grooth, B. G.; Segerink, F. B.; Schipper, E. H.; Hulst, N. F.; Greve, J. *Rev. Sci. Instr.* **1993**, *64*, 2892.
(10) Ruiter, A. G. T.; Veerman, J. A.; Garcia-Parajo, M. F.; van Hulst, N. F. *J. Phys. Chem. A* **1997**, *101*, 7318.
(11) Veerman, J. A.; Otter, A. M.; Kuipers, L.; van Hulst, N. F. *Appl. Phys. Lett.* **1998**, *72*, 3115.
(12) Huck, W. T. S.; van Veggel, F. C. J. M.; Kropman, B. L.; Blank, D. H. A.; Keim, E. G.; Smithers, M. M. A.; Reinhoudt, D. N. *J. Am. Chem. Soc.* **1995**, *117*, 8293.
(13) Huck, W. T. S.; van Veggel, F. C. J. M.; Reinhoudt, D. N. *J. Mater. Chem.* **1997**, *7*, 1213.
(14) Huck, W. T. S.; Snellink-Ruël, B. A.; van Veggel, F. C. J. M.; Lichtenberg, J. W. Th.; Reinhoudt, D. N. *Chem. Commun.* **1997**, *1* (9), 1359.
(15) Bethe, H. A. *Phys. Rev.* **1944**, *66*, 163.
(16) Bouwkamp, C. J. *Philips Res. Rep.* **1950**, *5*, 401.
(17) Novotny, L.; Pohl, D. W.; Hecht, B. *Ultramicroscopy* **1995**, *61*, 1.
(18) Betzig, E.; Chichester, R. J. *Science* **1993**, *262*, 1422.
(19) Veerman, J. A.; Garcia-Parajo, M. F.; Kuipers, L.; van Hulst, N. F. *J. Microscopy* **1999**, *194*, 477.
(20) Ha, T.; Enderle, Th; Chemla, D. S.; Selvin, P. R.; Weiss, S. *Phys. Rev. Lett.* **1996**, *77*, 3979.